

Evaluation of Biomedical Activity of ZnO Coated Bionanocomposites Film

^[1] Rebika Baruah *, ^[2] Archana Moni Das

^[1] CSIR-North East Institute of Science and Technology, Assam, India,

^[2] Academy of Scientific and Innovative Research (AcSIR), Ghaziabad, India.

Corresponding Author Email: ^[1] baruahrebika9@gmail.com*, ^[2] archanamoni@neist.res.in

Abstract— Bionanocomposites materials are the ideal alternative for petroleum-based products. They solve not only the global warming issue but also the problems of multidrug-resistant pathogens. We have synthesized a biopolymer-based ZnO nanocomposites film by using cellulose as supporting agent and the extract of *Livistona jenkinsiana* as reducing agents. We also utilized the antibacterial property of chitosan and superior delivery property of α -cyclodextrin in the synthesis of bionanocomposites. The new and novel cellulose/chitosan/ α -cyclodextrin/*Livistona jenkinsiana*/ZnO bionanocomposites film (CCCLZF) as a promising biomedical applicant was utilized for the first time. Several characteristics were performed to confirm the shape, size, structure, chemical composition, morphology, thermal properties, stability of the films, they are UV-Visible spectroscopy, FTIR spectroscopy, XRD pattern, SEM, and TEM images, EDS, TGA, DTA, DLS, and Zeta potential. To study the biomedical property of the CCCLZF; the antimicrobial, antioxidant, and anti-inflammatory activity of the film was examined. Drug delivery of the film was also investigated. All the experiments obtained good purposeful results. Therefore, CCCLZF will be a promising material in the pharmaceutical and food packaging industry.

Keywords— Bionanocomposites, films, nanoparticles, ZnO.

I. INTRODUCTION

Global warming is the serious issue in 21st century due to the burning of fossil fuels. Replacement of these harmful materials is urgent need for the human mankind. Bionanocomposites is an ideal candidate to replace the toxic materials and fulfill all the aspects of human. Due to biodegradability, biocompatibility, sustainability and economic nature of the bionanocomposites, they have remarkable application in various fields, especially biomedical field [1], [2].

Cellulose is the world's most abundant biopolymers. Due to the renewable property of cellulose, it can be used as ideal substitute in the place of non-biodegradable petroleum based products. In food packaging industry, cellulose based bionanocomposite films can be used as efficient packaging materials due to their improved mechanical, thermal, optical and barrier behavior [3]-[5].

Chitosan is a natural organic compound originated from chitin through deacetylation. Position of natural abundance of chitosan is second in the world among other biopolymer. The bionanocomposites containing chitosan offers excellent biological and physicochemical characteristics which make them an economic antibiotics and efficient adsorbent to prevent the growth of multi-drug resistant bacteria and to adsorb pollutants from polluted water respectively [6]-[10].

β -Cyclodextrin (β -CD) belongs to the class of non-reducing cyclic oligosaccharide. Due to the hydrophobic nature of the internal cavity β -CD, bionanocomposites consists of β -CD can be sufficiently applied in the delivery of hydrophobic drugs [11]-[13].

Metal oxide nanoparticles (NPs) are the efficient biomedical applicant due to its economic, eco-friendly and biocompatible nature. ZnO NPs are suitable candidate in this category. ZnO NPs is an efficient antibacterial and anticancer agent due to its excellent optical and biocompatible nature. Besides, this n-type semiconductor has tremendous application in other biomedical fields [14]-[16].

Livistona jenkinsiana belongs to the family Arecaceae. The leaves of the plants are rich in several bioactive molecules and possess notable biological activity in the controlling of severe diseases. The extracts of leaves can be applied against multidrug resistant pathogens and cancer cell lines. Therefore, extract of *Livistona jenkinsiana* is a potential material to reduce and cap the ZnO NPs [17].

In our study, we have synthesized *Livistona jenkinsiana* mediated ZnO NPs and incorporated them into biopolymer matrix of cellulose, chitosan and α -cyclodextrin for the first time. The novel and innovative bionanocomposites were characterized by different analytical tools such as UV-Visible spectroscopy (UV-Vis), Fourier-transform infrared spectroscopy (FTIR), X-ray diffractometer (XRD), Scanning electron microscope (SEM), Energy dispersive spectroscopy (EDS), Transmission electron microscope (TEM), Thermal gravimetric analysis (TGA), Differential thermal analysis (DTA), Dynamic light scattering (DLS) and Zeta potential analysis. Agar well diffusion method was applied to determine the antibacterial activity of the film and minimum inhibitory concentration (MIC) was also determined. Antioxidant activity of the film was screened by using DPPH assay. Anti-inflammatory activity and drug delivery of the cellulose/chitosan/ α -cyclodextrin/*Livistona jenkinsiana*/ZnO bionanocomposites film (CCCLZF) was also evaluated.

Ofloxacin was taken as a model drug in drug delivery application. Therefore, this biocompatible, economic and innovative bionanocomposites film is a promising material in biomedical field.

II. EXPERIMENTAL

1. Materials

All the chemicals used in the synthesis of bionanocomposites films and its application were purchased from Merk, TCI and Hi media chemicals and used as received. Double distilled H₂O was used for the preparation of solutions. Cellulose was extracted from *Livistona jekinsiana* leaves. The plant materials were collected from North-West Jorhat, Assam and washed thoroughly with distilled water to remove dust particles and impurities before the extraction of the leaves.

2. Analytical Methods

The optical properties of the ZnO NPs were examined by measuring the UV-Vis absorption of the NPs by using a UV-Vis spectrophotometer (Hitachi Model No –U-3900). FTIR spectroscopy (Perkin-Elmer FTIR-2000 spectrometer) was used to determine the action of phytochemicals in the synthesis of nanoparticles as reducing agents and the presence of biopolymer in the bionanocomposites films. X-ray diffractometer (Rigaku Ultima IV diffractometer) was employed to determine the crystalline nature and size and phase of the nanocomposites. The morphology and chemical composition of the composites film were determined by SEM images and EDS analysis respectively (ZEISS, SIGMA instrument). The phase, shape, and size of the synthesized ZnO NPs were analysed by the transmission electron microscope (JEM-2100 Plus). Zeta potential and DLS analysis was used to measure the stability and size distribution and polydispersity index of the ZnO NPs respectively (Nano ZS Zetasizer (Malvern)). Thermal properties of the nanocomposites films were studied by TGA and DTA analysis on SDT Q600 V20.9 Build 20. UV-Vis spectrophotometer was employed in the screening of antioxidant and anti-inflammatory activity and drug delivery ability of the nanocomposites film. The antimicrobial activity was determined by measuring zone of inhibition of every tested pathogens and MIC was also determined.

3. Preparation of the Extracts of *Livistona jekinsiana* Leaf

The cleaned leaves were cut in small pieces, sun-dried and grinded into powder form. 10 g of powdered leaves were added into 100 ml distilled H₂O in an Erlenmeyer flask and stirred at 60°C until the color of the extracts become brown. The brown extracts were collected by filtration followed by centrifugation to remove un-dissolved materials and stored at 4°C for purposeful application.

4. Preparation of Biopolymer Solution

4.1 Cellulose Solution

1 g of cellulose was dissolved in 8 g of LiOH and 15 g urea containing solution proposed by Cai *et al.* [18]. The cellulose solution was stored at 4°C for further application.

4.2 Chitosan Solution

Chitosan solution was determined by dissolving 1 g of chitosan in 1% acetic acid solution of water and the prepared solution was stored at 4°C for further application.

4.3 β-Cyclodextrin Solution

1g of β-Cyclodextrin was dissolved in 100 ml distilled H₂O and the solution was stored at 4°C for further application.

5. Synthesis of *Livistona jekinsiana* Mediated ZnO NPs (LJ-ZnO NPs)

LJ-ZnO NPs was synthesized by the methods proposed by us in previous publication with slight modification [19]. Briefly, 0.1 M of ZnNO₃ was added to 30 ml plant extract at pH 7. The mixture was stirred at 60°C for 1h. The transformation of brown color of the mixture to a dark yellow colloidal solution preliminary confirmed the formation of ZnO NPs and finally by the UV-Vis spectroscopy by measuring its characteristics absorption peak.

6. Synthesis of cellulose/ chitosan/ β-cyclodextrin/ *Livistona jekinsiana*/ZnO Bionanocomposites Film (CCCLZF)

10 ml of each biopolymer i.e. cellulose, chitosan and β-cyclodextrin was added to an Erlenmeyer flask to get a polymer solution. 10 ml of glycerol was used as plasticizer. The mixture was stirred at room temperature to get a clear solution. The clear solution was mixed with 0.250 g of LJ-ZnO NPs and kept under stirring for 2 h to get a clear solution of polymer and NPs. Solvent casting methods was employed to prepare the nanocomposites films. Then generated wet films were washed with distilled water to remove impurities. These wet films dried at room temperature.

7. Antimicrobial Activity of CCCLZF

Agar well diffusion method was employed to evaluate the antimicrobial activity of CCCLZF. For the experiment, four bacterial strain namely, *Bacillus subtilis* (MTCC 441), *Escherichia coli* (ATCC 11229), *Staphylococcus aureus* (ATCC 11682), *Klebsiella pneumoniae* (ATCC 13883), and one fungal strain *Candida albicans* (MTCC 3017) was selected. For antimicrobial experiment, Mueller Hinton agar and broth (MHA and MHB) and Potato Dextrose agar and broth (PDA and PDB) were used as media. Cultured microbes were streaked on sterilized agar using a sterilized spreader. By using a sterilized borer, well of 6 mm was made on agar. The film of 6 mm containing different concentration of LJ-ZnO NPs (20, 40, 60, 80, and 100 µg/ml) was placed in well. Neomycin and nystatin was used as antibacterial standard and antifungal standard respectively. Incubation

time of bacteria and fungi contained Petri dishes was 12 and 24 h respectively at 37°C. Inhibition ability of nanocomposites film towards the growth of experimental pathogens was examined by measuring the zone of inhibition in millimeter (mm).

7.1. Minimum Inhibitory Concentration (MIC)

MIC of CCCLZF was determined by broth dilution method. MHB and PDB were used as media. Different concentration (5, 15, 25, 35, 45, 55, 65, 75, 85, and 95µg/ml) of NPs containing mixture of biopolymer and NPs was mixed with 2 ml of fresh cultured microbes (approximately 10⁶CFU/ml). Negative control was the test tube filled with only broth and inoculum. Incubation time for the test tubes with bacterial and fungal strains inoculation were 24 hr at 37°C and 30°C for 48 h respectively. The minimum concentration of NPs containing biopolymer mixture which inhibited the growth of pathogens over 85% is considered as a MIC of CCCLZF.

8. Antioxidant Activity of CCCLZF

8.1. DPPH Radical Scavenging Assay

DPPH radical scavenging assay was employed to determine the antioxidant activity of the CCCLZF. Antioxidants can reduce the stable free radical DPPH (2, 2-diphenyl-1-picrylhydrazyl). 2ml of different concentrations (20, 40, 60, 80 & 100µg/ml) of NPs with biopolymer solution and standard (ascorbic acid) were taken in a test tube and the stock solutions were mixed with 1ml of DPPH (.1mM of 20 ml ethanolic solution) solution. 30% ethanolic solution was considered as blank in the measurement of absorption of DPPH solution containing different concentrations of nanocomposites. DPPH solution without NPs and standard was considered as a negative control.

The DPPH free radical scavenging activity was determined using the following formula:

$$\% \text{ scavenging} = \left[\frac{\text{Absorbance of control} - \text{Absorbance of test sample}}{\text{Absorbance of control}} \right] \times 100$$

9. Anti-inflammatory Activity of CCCLZF

Anti-inflammatory activity of the CCCLZF was screened in vitro. Anti-inflammatory activity of the film determined the inhibition power towards protein denaturation. 50 ml of different concentration of NPs containing polymer solution was added with 5 ml of 0.2% (w/v) BSA solution. The mixture was heated at 72°C for 5 min and cooled for 10 min. Control of the assay was considered as 5 ml of 0.2% w/v BSA solution with 50 ml water. Diclofenac (100 mg/ml) in water with 5 ml 0.2% w/v BSA solution was used as standard. Inhibition ability was measured by taking the absorbance of different concentrations of NPs containing solutions at 276 nm. IC₅₀ values were determined to determine the concentration that showed 50% inhibition ability.

10. Drug Delivery action of CCCLZF

Drug release ability of CCCLZF was determined by taking ofloxacin as a model drug. 0.2 g of film was equilibrated in 20 ml of drug solution (100 ppm in distilled water) at 25°C for 2 days. Loading of the drug in to the films was determined by the taking absorption of the drug containing solution at 293 nm with the help of UV-Vis spectroscopy. Content of drug in the film was calculated by using following equation.

$$\% \text{ Drug Loading} = \left(\frac{\text{Weight drug in a sample}}{\text{Weight of sample taken}} \right) \times 100$$

Drug release ability of nanocomposites films was determined at pH 7.4 for 24 h. Experimentally, 0.2 g drug-loading film was kept in 10 ml of buffer solution (pH 7.4). Release medium was kept at room temperature under constant stirring of 50 rpm. Equal amounts of investigated drug containing solution were picked up at regular time interval. Amount of drug in the collected samples were determined by taking the absorption of the samples by UV-Vis spectroscopy. Collected samples from stirred drug containing solution were replaced by fresh buffer solution to maintain the volume of the experimental solution constant. Standard calibration curve was applied to determine the quantity of ofloxacin release by nanocomposites film.

III. RESULTS AND DISCUSSION

3.1. Optical Nature of LJ-ZnO NPs

The UV-Vis absorption spectrum of LJ-ZnO NPs showed the formation of an absorption peak at 352 nm, which was consistent with previous studies and confirmed the formation of NPs. The absorption peak is due to surface plasmon resonance. The difference in the absorption peak from the absorption of bulk ZnO (378 nm) is due to quantum confinement effect (Fig. 1). The band gap of the NPs was determined by $E_g = 1240/\lambda$, it was 3.52.

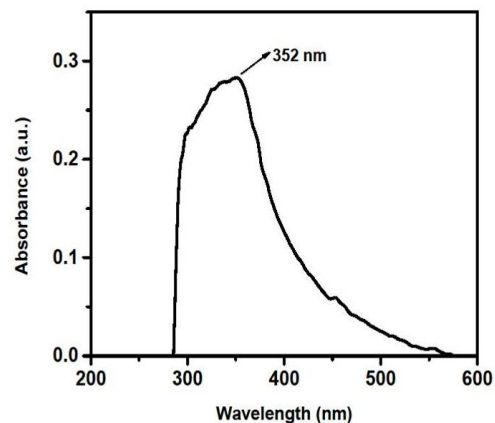


Fig. 1: UV-Vis spectrum of the LJ-ZnO NPs.

3.2. Crystalline Nature of CCCLZF

The XRD pattern of CCCLZF was determined the crystalline structure of the film. XRD pattern showed characteristic peaks corresponding to the planes (1 0 0) at $2\theta = 32.34^\circ$, (0 0 2) at $2\theta = 35.1^\circ$, (1 0 1) at $2\theta = 36.8^\circ$, (1 0 2) at $2\theta = 47.7^\circ$, (1 1 0) at $2\theta = 56.2^\circ$, (1 0 3) at $2\theta = 62.3^\circ$ and (1 1 2) at $2\theta = 67.6^\circ$ (Fig.2). Characteristics peaks of the film revealed the close packed hexagonal Wurtzite structure of ZnO. Incorporation of NPs into the biopolymer matrix was ascertained by the intense peak around 20.9° (0 0 2). Hence, the results obtained from XRD pattern of CCCLZF approved the presence of LJ-ZnO NPs in the biopolymers matrix with uniform size.

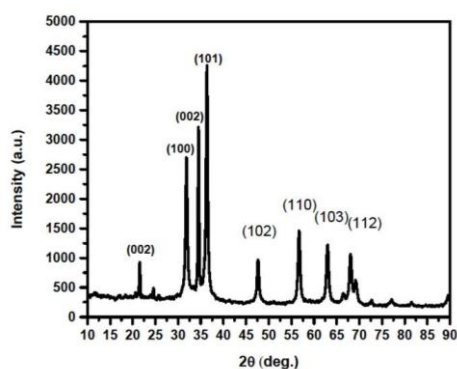


Fig. 2: XRD patterns of CCCLZF.

3.3. FTIR Analysis

Incorporation of LJ-ZnO NPs in the biopolymer matrix and participation of phytochemicals in the synthesis of ZnO NPs were revealed by FTIR spectrum of CCCLZF (Fig. 3). OH and CH_2 asymmetric stretching of biopolymer was ascertained by the presence of FTIR absorption bands at 3399.76 and 2919.64 cm^{-1} respectively. The bands correlated to $\text{C}=\text{O}$ stretching vibrations of amide I and amide II appeared at 1647.55 cm^{-1} . FTIR bands at 1584 cm^{-1} corresponded to N-H bending vibrations of NH_2 . The band ascribed with CH_2 wagging coupled with OH group from CH appeared at 1384.75 cm^{-1} . The absorption band at 578.78 cm^{-1} corresponded to the Zn-O bind in the LJ-ZnO NPs.

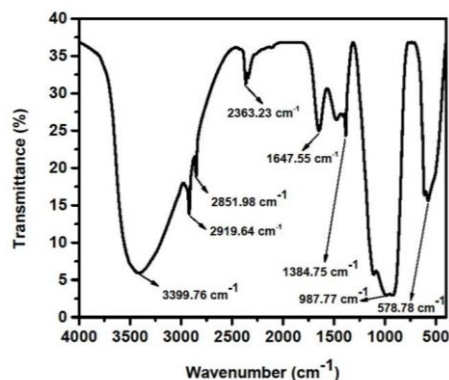


Fig. 3: FTIR spectrum of CCCLZF.

3.4. Morphology, Shape and Elemental Composition of CCCLZF

SEM images of CCCLZF were utilized to determine the morphology and shape of the nanocomposites film (Fig. 4 (a)). Uniform, spherical shape and uniform distribution of the LJ-ZnO NPs was revealed by SEM images. These characteristics made film efficient for biomedical application. SEM images showed that there was no severe agglomerations of ZnO NPs in the biopolymer matrix which helped in the uniform distribution of the LJ-ZnO NPs. Simultaneously, EDS analysis of the CCCLZF confirmed the presence of LJ-ZnO NPs in the prepared bionanocomposites film (Fig. 4 (b)).

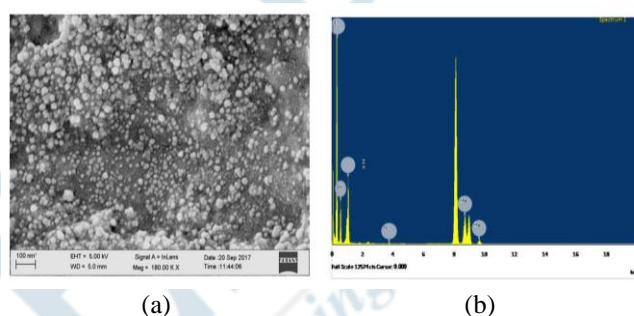


Fig. 4: SEM images and EDS pattern of CCCLZF.

3.5. TEM Analysis

TEM images determined the shape and size of the LJ-ZnO NPs in the biopolymer matrix (Fig. 5(a)). There was some agglomeration in between the uniformly distributed spherically shaped ZnO NPs and the agglomeration was due to the aqueous medium of the synthesis. The size of the NPs was 40-50 nm. In HRTEM of ZnO NPs, the fringe spacing was 0.25 nm corresponded to (002) plane of the wurtzite structure of the ZnO NPs (Fig. 5 (b)). Results of XRD pattern were similar with the SAED pattern by correlating the planes (002) and (110) (Fig. 5 (c)).

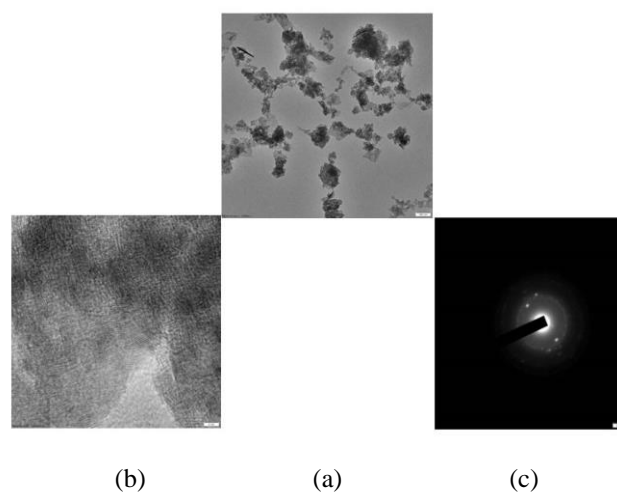


Fig. 5: TEM images (a), HRTEM (b) and SAED pattern (c) of CCCLZF.

3.6. TGA and DTA analysis

TGA and DTA curve of the CCCLZF exhibited 4% weight loss at 600°C and thermal decomposition at 530°C, respectively (Fig. 6 (a) & (b)).

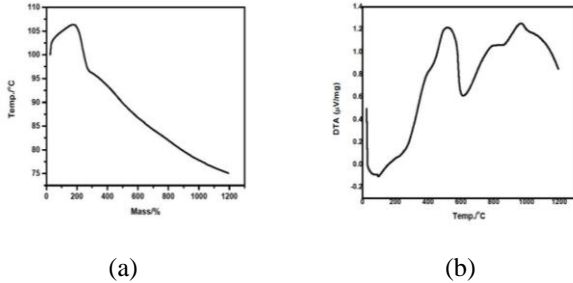


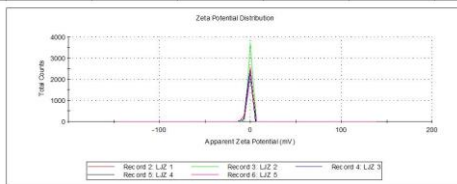
Fig. 6: TGA and DTA of CCCLZF.

3.7. Zeta Potential and DLS Analysis

Zeta potential of CCCLZF determined the stability of the LJ-ZnO NPs in the biopolymer matrix. The value of average zeta potential of ZnO NPs was 3.34 mV with a standard deviation of 1.23. Zeta potential value determines the repulsive force between the NPs. This zeta potential value depicted the moderate stability of the NPs with low agglomeration (Fig. 7 (a)).

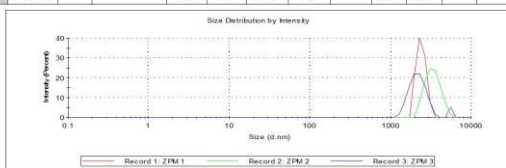
DLS analysis revealed the average size of the LJ-ZnO NPs. The average size was 3661.33 nm with a standard deviation of 393.75. TEM and DLS analysis gave different size of same LJ-ZnO NPs due to the solvation effect of DLS analysis [20]. Polydispersity Index (PDI) of ZnO NPs was found to be 0.306 with a standard deviation of 0.084 (Fig. 7 (b)).

Sample Name	No. of Times	Temperature (°)	Zeta Potential mV	Mobility μmcm/Vs	Conductivity mS/cm	Wall Zeta Potential mV
ZnO NCS	1	25	-0.381	-0.02987	1.41	3.2
	2	25	0.202	-0.01587	1.45	4.63
	3	25	-0.314	-0.02463	1.48	2.18
	Std Dev 1-3	0	0.319018	0.025033	0.028284	1.23



(a)

Sample	No. of Times	Type	Temperature (°)	Z-Ave d.nm	PDI	Pk1 Mean Int d.nm	Pk2 Mean Int d.nm	Pk3 Mean Int d.nm	Pk1 Area Int %	Pk2 Area Int %	Pk3 Area Int %	Aggre Index	Scat. Ang. (°)
ZnO NCS	1	Size	25	3220	0.362	2414	0	0	100	0	0	0	173
	2		25	3882	0.209	3407	0	0	100	0	0	0	173
	3		25	3882	0.347	2193	5560	0	94.8	5.2	0	0	173
	Std Dev 1-3	0	383.7	0.084	646.6	339	3210	0	3.00	3.00	2221	0	0



(b)

Fig. 7: Zeta potential (a) and (b) Of CCCLZF.

3.8. Antimicrobial Activity of CCCLZF

CCCLZF showed potential antimicrobial activity against gram-positive and gram-negative bacteria and fungi (Fig. 8). The nanocomposites film efficiently inhibited the growth of pathogens and acted as promising antimicrobial agents in the controlling of various severe diseases.

Table I and II illustrated the diameter of inhibition zone of experimental pathogens in the presence of CCCLZF. ZnO NPs were more sensitive to gram-positive bacteria than gram-negative one. The difference was due to the different structural composition of cell wall of the gram-positive and gram-negative bacteria. High stability and high surface to volume ratio of the LJ-ZnO NPs in the biopolymer matrix made the nanocomposites film efficient antibiotics as compared to bulk ZnO. Like bacteria, CCCLZF successfully inhibit the growth fungi also (TableII).

Table 1. Antifungal activity of CCCLZF.

S No.	Test Organisms	Zone of Inhibition (in mm) for different concentrations of CCCLZF					Nystatin (Standard) (ZI) ^b
		1	2	3	4	5	
1	<i>C. albicans</i>	0	9± 0.1	10± 0.8	11± 0.8	13± 0.8	26± 0.5

Table 2. Antibacterial activity of CCCLZF.

S No.	Test Organisms	Zone of Inhibition (in mm) for different concentrations of CCCLZF					Neomycin (Standard) (ZI) ^b
		1	2	3	4	5	
1	<i>S. aureus</i>	11±0.1	12± 0.4	13± 0.3	14± 0.6	16± 0.5	26± 0.5
2	<i>E. coli</i>	0	9± 0.0	10± 0.0	13± 0.2	12± 0.2	26± 0.6
3	<i>B. subtilis</i>	10±0.8	12± 0.8	14± 0.3	16± 0.9	18± 0.7	22± 0.4
4	<i>K. pneumonia</i>	9±0.8	10± 0.2	11± 0.0	12± 0.2	13± 0.0	22± 0.5

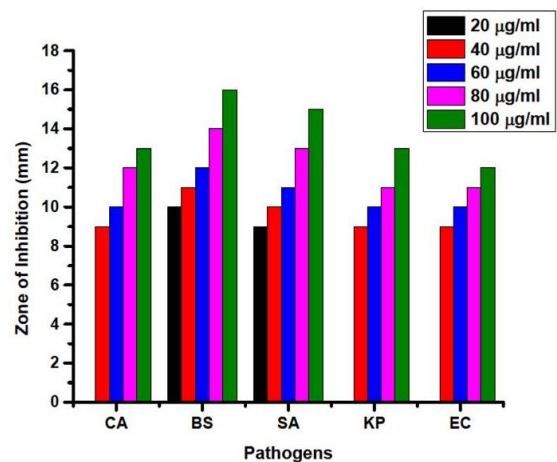


Fig. 8: Antimicrobial activity of CCCLZF.

3.8.1. MIC

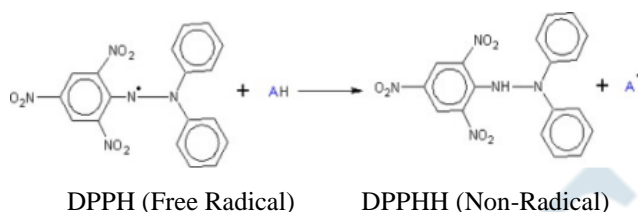
Table III illustrated the minimum concentration of LJ-ZnO NPs in the biopolymer matrix that effectively inhibit the 85% growth of pathogens. The lower MIC value revealed that CCCLZF will be an ideal substituent to prevent the transmission of diseases by multidrug resistant microbes for the conventional medicine.

Table 3. The MIC of CCCLZF.

Bacterial strains	MIC($\mu\text{g/mL}$)
<i>S. aureus</i>	25
<i>E. coli</i>	35
<i>B. subtilis</i>	20
<i>K. pneumonia</i>	35
<i>C. albicans</i>	25

3.9. Antioxidant Activity

The IC₅₀ value of the CCCLZF was determined to screening the antioxidant activity of the film. IC₅₀ value was found to be 124.45 $\mu\text{g/ml}$. Small size and large surface area of the ZnO NPs in the biopolymer matrix made the film effective to interact and reduce DPPH. According to the equation mentioned below DPPH reduced to DPPHH (Fig. 9 (a)).



3.10. Anti-inflammatory Activity

Anti-inflammatory activity of the CCCLZF was determined by interpreting the IC₅₀ value of LJ-ZnO NPs in the biopolymer matrix. IC₅₀ value was 96.78 $\mu\text{g/ml}$ and the low value was due to the extra small size, stability and large surface area of ZnO NPs in nanocomposites film. Standard in anti-inflammatory activity was Diclofenac that exhibited 62.55 $\mu\text{g/ml}$ IC₅₀ value, (Fig. 9 (b)).

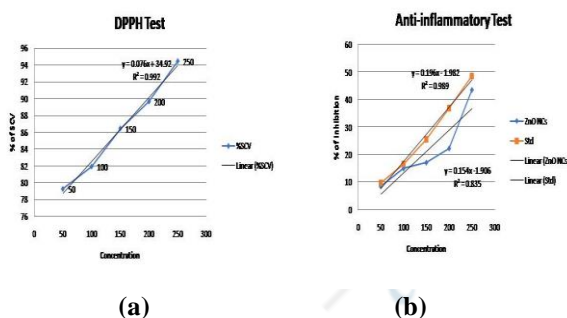


Fig. 9: Antioxidant (a) and anti-inflammatory (b) activities of CCCLZF.

3.11. Drug Release Properties of CCCLZF

The amounts of ofloxacin loaded on CCCLZF and fractional release of the drug from nanocomposite films were calculated. Prolonged drug release behavior was due to the efficacy of LJ-ZNO NPs in the biopolymer matrix in case of drug loading. Extending release time of ofloxacin from CCCLZF revealed that model drug cross a longer path from CCCLZF to the buffer solution for mitigation. The drug loading capacity was 34.50% and encapsulation efficiency

was 29.78%.

IV. CONCLUSION

Novel bionanocomposites film based on cellulose, chitosan, β -cyclodextrin and LJ-ZnO NPs were successfully prepared. Different characteristics of CCCLZF were evaluated by using different analytic tools. UV-Vis spectra of the ZnO NPs confirmed the formation of NPs. FTIR revealed the participation of phytochemicals in the synthesis of ZnO NPs and incorporation of biopolymer in CCCLZF. XRD confirmed the crystalline structure and phase of the CCCLZF. SEM and TEM images determined the morphology of the CCLJF and size of the LJ-ZnO NPs. TGA and DTA confirmed the thermal stability of the CCCLJF. Zeta potential revealed the stability of the NPs in the biopolymer matrix. The efficient antimicrobial, antioxidant, anti-inflammatory and drug delivery activities of the CCCLZF proved that this novel and innovative bionanocomposites films will be a promising material in food packaging and pharmaceutical industry.

Acknowledgments

The Director of CSIR-North East Institute of Science and Technology, Jorhat, Assam gave permission to carry out our research with excellent facilities. Therefore, R. Baruah and A. M. Das sincerely offer their heartfelt gratitude to him. Department of Science and Technology (DST), New Delhi, grant the Fellowship to R. Baruah (GAP-0754). So, she is sincerely thankful to DST, India.

REFERENCES

- [1]. R. A. Ilyas, S. M. Sapuan, M. R. Ishak, and E. S. Zainudin, "Water Transport Properties of Bio-Nanocomposites Reinforced by Sugar Palm (*Arenga Pinnata*) Nanofibrillated Cellulose," J. Adv. Res. Fluid Mech. Therm. Sci., vol. 51, no. 2, pp. 234-246, November 2018.
- [2]. M. Alavi, N. Karimi, and I. Salimikia, "Phytosynthesis of zinc oxide nanoparticles and its antibacterial, antiquorum sensing, antimotility, and antioxidant capacities against multidrug resistant bacteria," J. Ind. Eng. Chem., vol. 72, pp. 457-473, April 2019.
- [3]. S. Thomas, J. Kuruvilla, and S.K. Malhotra, "Electrical and optical studies of organic light emitting devices using SWCNTs-polymer nanocomposites," Polym. Compos. Biocompos., Vol. 3, pp. 1-608, January 2013.
- [4]. E. Ruiz-Hitzky, M. Darder, and P. Aranda, in: E. Ruiz-Hitzky, K. Ariga, Y.M. Lvov (Eds.), Bio-Inorganic Hybrid Nanomaterials, Wiley-VCH, Weinheim, pp. 1-40, December 2007.
- [5]. J.W. Rhim, H.M. Park, C.S. Hac, "Bio-nanocomposites for food packaging applications," Prog. Polym. Sci., vol. 38, pp. 1635-1689, October-November 2013.
- [6]. M.C. Maria, K. Kaviyarasu, and A. Raja, "Photocatalytic decomposition effect of erbium doped cerium oxide nanostructures driven by visible light irradiation: investigation of cytotoxicity, antibacterial growth inhibition using catalyst," J Photochem Photobiol B Biol., Vol. 185, pp. 275-282, August 2018.

- [7]. Z.A.M. Kebir, M. Adel, and M. Adjdir, "Preparation and antibacterial activity of silver nanoparticles intercalated kenyaite materials," *Mater Res Express.*, Vol. 5, pp. 085021, July 2018.
- [8]. H.L. Su, C.C. Chou, and D.J. Hung, "The disruption of bacterial membrane integrity through ROS generation induced by nanohybrids of silver and clay," *Biomaterials*, vol. 30, no. 30, pp. 5979-5987, October 2009.
- [9]. S.P. Raut, R.V. Ralegaonkar, and S.A. Mandavgane, "Development of sustainable construction material using industrial and agricultural solid waste: a review of waste-create bricks," *Constr Build Mater.*, Vol. 25, no. 10, pp. 4037-4042, October 2011.
- [10]. M. Rinaudo, "Chitin and chitosan: properties and applications," *Prog Polym Sci.*, vol. 31, no. 7, pp. 603-632, July 2006.
- [11]. A. Gogoi, and K.C. Sarma, "Synthesis of the novel β -cyclodextrin supported CeO₂ nanoparticles for the catalytic degradation of methylene blue in aqueous suspension," *Mater. Chem. Phys.*, vol. 194, pp. 327-336, July 2017.
- [12]. M. E. Navgire, P. Gogoi, and B. Mallesham, " β -Cyclodextrin supported MoO₃-CeO₂ nanocomposite material as an efficient heterogeneous catalyst for degradation of phenol," *RSC Adv.*, vol. 6, pp. 28679-28687, March 2016.
- [13]. F.J. Otero-Espinar, J.J. Torres-Labandeira, and C. Alvarez-Lorenzo, "Cyclodextrins in drug delivery systems," *J. Drug Deliv. Sci. Technol.*, vol. 20, no. 4, pp. 289-301, 2010.
- [14]. M. S. Geetha, H. Nagabhushana, and H. N. Shivananjaiiah, "Green mediated synthesis and characterization of ZnO nanoparticles using *Euphorbia jatropha* latex as reducing agent," *J SCI: ADV MATER DEV*, vol. 1, no. 3, pp. 301-310, September 2016.
- [15]. G. Sangeetha, S. Rajeshwari, and R. Venckatesh, "Green synthesis of zinc oxide nanoparticles by *Aloe barbadensis miller* leaf extract: Structure and optical properties," *Mater. Res. Bull.*, vol. 46, no. 12, pp. 2560-2566, December 2011.
- [16]. A. Happy, S. V. Kumar, and S. Rajeshkumar, "A review on green synthesis of zinc oxide nanoparticles – An eco-friendly approach," *Resource-Efficient Technologies*, vol. 3, no. 4, pp. 403-417, December 2017.
- [17]. R. K. Singh, R. C. Srivastava, T. K. Mukherjee. "Toko-Patta (*Livistona jenkinsiana* Griff): *Adi* community and conservation of culturally important endangered tree species in eastern Himalaya," *Indian J. Tradit. Knowl.*, vol. 9, pp. 231-241, April 2010.
- [18]. J. Cai, and L. Zhang, "Rapid dissolution of cellulose in LiOH/urea and NaOH/urea aqueous solutions," *Macromol Biosci.*, vol. 5, no. 6, pp. 539-48, June 2005.
- [19]. R. Baruah, A. Yadav, and A.M. Das, "*Livistona jenkinsiana* fabricated ZnO nanoparticles and their detrimental effect towards anthropogenic organic pollutants and human pathogenic bacteria," *SPECTROCHIM ACTA A.*, vol. 251, pp. 119459, April 2021.
- [20]. H. Lee, Y. K. Park, S. J. Kim, B. H. Kim, H. S. Yoon, and S. C. Jung, "Rapid degradation of methyl orange using hybrid advanced oxidation process and its synergistic effect," *J. Ind. Eng. Chem.*, vol. 35, pp. 205-210, March 2016.